A Letters Journal Exploring the Frontiers of Physics

January 2014

EPL, **105** (2014) 20001 www.epljournal.org
doi: 10.1209/0295-5075/105/20001

Chaoticity without thermalisation in disordered lattices

O. Tieleman[1], Ch. Skokos[1,2,3] and A. Lazarides[1]

[1] *Max-Planck-Institut für Physik komplexer Systeme - Nöthnitzer Straße 38, D-01187 Dresden, Germany*
[2] *Physics Department, Aristotle University of Thessaloniki - GR-54124, Thessaloniki, Greece*
[3] *Department of Mathematics and Applied Mathematics, University of Cape Town - Rondebosch, 7701, South Africa*

received 8 August 2013; accepted in final form 8 January 2014
published online 6 February 2014

PACS 03.75.Hh – Static properties of condensates; thermodynamical, statistical, and structural properties
PACS 05.45.-a – Nonlinear dynamics and chaos
PACS 67.85.-d – Ultracold gases, trapped gases

Abstract – We study chaoticity and thermalization in Bose-Einstein condensates in disordered lattices, described by the discrete nonlinear Schrödinger equation (DNLS). A symplectic integration method allows us to accurately obtain both the full phase space trajectories and their maximum Lyapunov exponents (mLEs), which characterize their chaoticity. We find that disorder destroys ergodicity by breaking up phase space into subsystems that are effectively disjoint on experimentally relevant timescales, even though energetically, classical localisation cannot occur. This leads us to conclude that the mLE is a very poor ergodicity indicator, since it is not sensitive to the trajectory being confined to a subregion of phase space. The eventual thermalization of a BEC in a disordered lattice cannot be predicted based only on the chaoticity of its phase space trajectory.

Introduction. – In this letter, we bring together the topics of disorder, nonlinearity, chaos, ergodicity, and Bose-Einstein condensation (BEC) in optical lattices. Inspired by the realisation of disordered optical potentials in experiments with ultracold atomic gases [1,2], we explore the question of thermalisation in such systems. Previous theoretical works have, amongst others, addressed the topics of Bose and Anderson glasses [3], Anderson localisation [4,5], and Lifshits glasses [6]. In [6], various regimes of interaction strengths were investigated, and it was found that for sufficiently strong interactions, a disordered BEC is expected. We will focus on this regime, and study the one-dimensional (1D) Bose-Hubbard model [7,8], which describes a bosonic gas in a lattice, in the mean-field approximation. The resulting model can be obtained by discretising the Gross-Pitaevskii equation, and is also known as the discrete nonlinear Schrödinger equation (DNLS) [9]. In this letter, we pose and answer the following question: what is the effect of disorder on thermalisation and ergodicity in the mean-field Bose-Hubbard model/DNLS?

The connection between chaoticity and thermalisation was recently discussed in the disorder-free case [10]. A natural question that arises in this context is: what happens to this connection when disorder is added to the system? Intuitively, one would expect chaotic trajectories to thermalise, since unlike regular ones, they are not confined to the neighborhood of stable periodic orbits. Not being confined, the expectation is that they are able to cover the available phase space, and that the system is therefore well described by the microcanonical ensemble, since only the energy and particle number are conserved. We demonstrate that this expectation is not correct by showing the existence of trajectories that, in spite of their chaotic nature, do not uniformly explore all energetically available phase space of the system. Since the energies involved are higher than the disorder potential, classical localisation cannot be responsible for this effect.

The most commonly employed method of chaos detection, which quantifies the sensitive dependence on initial conditions, is the evaluation of the maximum Lyapunov exponent (mLE) [11–14]. In [10], a positive mLE, which indicates a chaotic trajectory, was found to predict thermalisation. To test this hypothesis in the disordered case, we investigate whether trajectories classified as chaotic based on the value of their mLE can be confined to subregions of phase space. Based on numerical studies of the disordered DNLS model, we find that generally, the mLE does not have any predictive power concerning spatial confinement of trajectories. Hence, we conclude that the mLE is not sufficient to answer such questions, since it

only tells us whether trajectories behave chaotically in a local sense. To the best of our knowledge, no studies addressing this question of confinement and chaoticity in disordered systems have been done hitherto. Confined trajectories are manifestly not ergodic, and therefore do not correspond to thermalising systems. Consequently, we find that in the presence of disorder, the connection between chaoticity and thermalisation is broken. Eventual thermalisation cannot be predicted based on the mLE alone; it has to be supplemented with at least one other quantity, which characterises the degree of confinement of the trajectory.

An important aspect of our system is the interplay between disorder and nonlinearity, which has been studied extensively in recent years [15–29] (see also sect. 7.4 in [30]). Most of these studies were concerned with the evolution of initially localized wave packets. It has been shown that for moderate values of nonlinearity the wave packets' second moment m_2 grows subdiffusively in time t, as t^α with $0 < \alpha < 1$ [18]. For weak enough nonlinearities, wave packets appear to be frozen for very long time intervals (whose duration increases as nonlinearity decreases) in a manner resembling Anderson localization. For very strong nonlinearities the existence of self-trapping behavior was theoretically predicted [17] and numerically verified [18,19,24–26] for the DNLS model, *i.e.* a part of the wave packet remains localized while the rest spreads subdiffusively. In our study, Anderson localisation plays an important role in understanding the physics.

System. – The Hamiltonian for the 1D disordered DNLS is given by

$$H = \sum_j \left[-J\left(\psi_j^* \psi_{j+1} + \text{h.c.}\right) + \varepsilon_j |\psi_j|^2 + \frac{\beta}{2}|\psi_j|^4 \right], \quad (1)$$

with site index j, complex wave function ψ_j, hopping strength J, on-site disorder $\varepsilon_j \in [-W/2, W/2]$, and nonlinear interaction strength β. We apply periodic boundary conditions. The quadratic part of the Hamiltonian can be written in diagonal form in the basis of its *normal modes*, which are all exponentially localised in the presence of disorder —this is the phenomenon of Anderson localisation [4]. The localisation length ξ varies within the band, but is bounded: $\xi \lesssim 96(J/W)^2$ [31]. The eigenenergies of the quadratic part lie in the interval $[-zJ - W/2, zJ + W/2]$, yielding a bandwidth of $2zJ + W$, where z is the number of neighbours per site (2, in our case). The importance of the interaction term is quantified by the nonlinearity parameter

$$\kappa = (\bar{n}\beta)/(J + W/2z), \quad (2)$$

where $\bar{n}$ is the average density: $\bar{n} = (1/L)\sum_j |\psi_j|^2$ in a system of L sites. Note that κ reduces to the interaction/kinetic ratio $\bar{n}\beta/J$ in the nondisordered case. The coupling between the normal modes due to the interaction term is proportional to the overlap integral $I_{\alpha\beta\gamma\delta} = \sum_j \phi_{\alpha,j}\phi_{\beta,j}\phi_{\gamma,j}\phi_{\delta,j}$, where $\phi_{\alpha,j}$ is the value of the αth eigenvector of the noninteracting Hamiltonian at site j. In the limit where the normal modes are each localised on a single site and $\phi_{\alpha,j} = \delta_{j,j_\alpha}$, this coupling vanishes. Thus, the expansion rate of a localised configuration can be extremely slow, much slower than any other process in the system, for small enough ξ. In such a case, the system effectively breaks up into uncoupled sites with a fixed on-site energy, on all other physically interesting timescales. We measure the degree of localisation by the participation fraction (PF) ϕ, which is defined as

$$\phi(\vec{\psi}) = \frac{1}{L}\frac{\sum_j |\psi_j|^2}{\sum_j |\psi_j|^4}. \quad (3)$$

It indicates the fraction of sites occupied in a state, as its extreme values are $\phi = 1/L$ for single-site occupation and $\phi = 1$ for equipartition.

Methods. – To obtain the evolution of a state under the Hamiltonian (1), we numerically integrate the coupled ordinary differential equations obtained from differentiating the Hamiltonian, $i\dot{\psi}_j = \partial H/\partial \psi_j^*$:

$$i\dot{\psi}_j = -J\left(\psi_{j+1} + \psi_{j-1}\right) + \varepsilon_j \psi_j + \beta |\psi_j|^2 \psi_j, \quad (4)$$

by means of a fourth order symplectic integration scheme explicitly developed for Hamiltonian systems that split in exactly three integrable parts [32,33]. Symplectic integrators are numerical techniques especially designed for the integration of Hamiltonian systems, keeping the error of the computed value of the energy bounded irrespectively of the total integration time (see, for example, chapt. VI of [34], [35,36] and references therein). Then we calculate the corresponding mLE using the so-called "standard method" [12,14] which is based on the time evolution of small deviations from the studied state. The mLE is defined as

$$\lambda(\vec{\psi}) = \lim_{\vec{\psi}'(0)\to\vec{\psi}(0)} \lim_{t\to\infty} \frac{1}{t} \ln \frac{|\vec{\psi}(t) - \vec{\psi}'(t)|}{|\vec{\psi}(0) - \vec{\psi}'(0)|}, \quad (5)$$

where $\vec{\psi}(t)$ represents a state at time t, and $|\vec{\psi}| = \sum_j |\psi_j|^2$. The mLE measures the dependence of the trajectory on the initial conditions: a positive value for λ indicates that trajectories that start out nearby diverge exponentially fast, indicating chaos, whereas for regular (nonchaotic) motion, the mLE is zero. Following [37] (see also [14] for more details) we linearize the equations of motion and obtain the so-called variational equations which govern the time evolution of a deviation vector $\vec{\psi} - \vec{\psi}'$. The deviation vector is initialised to point in a random direction and have unit norm. Integrating the variational equations along the trajectory obtained from the full equations of motion then allows us to calculate the growth of the Euclidean distance, and finally the mLE. This integration is achieved by an extension of the symplectic integrator according to the so-called "tangent map method" [38,39]. As initial condition, we have used the (noninteracting) ground state of

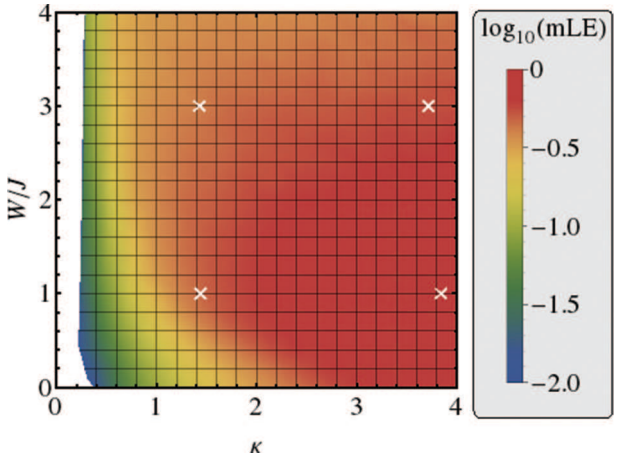

Fig. 1: (Colour on-line) The logarithm of the mLE as a function of the disorder strength W/J and nonlinearity parameter κ. The white crosses indicate the parameter values for the four sets of runs shown in fig. 2. The white region on the left features very low values for $\log_{10}$ mLE, since the mLE vanishes when $\kappa \to 0$ (see text).

the disordered potential combined with a harmonic trap, *i.e.* the lowest-energy normal mode of the combined potential $V_j = \varepsilon_j + [(j - L/2)/l_{\rm trap}]^2$, where $l_{\rm trap} \approx 30$. The density S was normalised to unity, *i.e.* $S = \sum_j |\psi_j|^2 = 1$. The trap was switched off before calculating the evolution, leaving only the disordered potential. Our model has two integrals of motion, as it conserves both the energy (1) and the norm S.

We have generated 100 random disorder realizations, calculated the appropriate initial condition for each realisation and value of W, and eventually averaged the mLE outcomes over the different realisations. The results presented here were obtained using a lattice of $L = 50$ sites, but the same behaviour was found on lattices up to 500 sites. Each case was integrated up to $t = 10^5 \hbar/J$. In all our computations the absolute value of the relative energy and norm error was kept smaller than 10^{-3}.

Since the tunnelling time is typically a few milliseconds, our integration time of $t = 10^5 \hbar/J$ corresponds to hundreds of seconds, while experiments usually do not last longer than a few seconds [40]. Our lattice size is also a typical value for experiments. The experimental tunability of the lattice depth via laser power, and atom-atom interaction via Feshbach resonances [41], allow for the exploration of a wide range of disorder strenghts and nonlinearities.

Results. – The disorder-averaged mLE at $t = 10^5$ tunnelling time units is shown in log-scale in fig. 1. It increases with the interaction strength β; this may be understood as follows. If the coupling β vanishes, the Hamiltonian becomes quadratic, and only regular orbits are expected. Switching on interactions induces mixing between the normal modes, and therefore departure from the regular orbits; the higher β, the stronger the mixing and the less regular/more chaotic the trajectories.

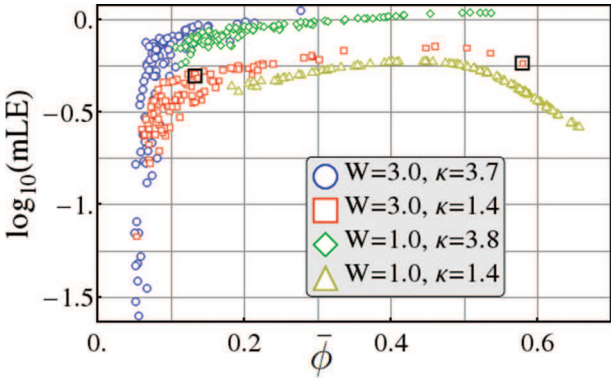

Fig. 2: (Colour on-line) The mLE and time-averaged PF of each of the 100 runs for four combinations (W, κ); W is given in units of J. The PF has been averaged over the last 10% of the run, to smooth out fluctuations (see, *e.g.*, the lower panel of fig. 3). Two runs are marked by (black) boxes; the time evolution of their PF and density distribution is plotted in fig. 3.

The mLE has a nonmonotonic behaviour as a function of the disorder strength, *i.e.* along vertical lines in fig. 1. The increase for weak disorder is a consequence of our choice of initial condition: increasing the disorder strenght increases the degree of localisation of the initial condition, which in turn leads to a higher energy and a larger energy shell. The larger enery shell facilitates divergence between initially neighbouring trajectories. This effect persists longer for weak interactions, where the growth of the energy shell as a function of W is slower. For strong enough disorder, any increase leads to a decrease in the mLE, which, as discussed earlier, can be understood as a localisation effect. While all orbits we found at nonzero β were chaotic, the range of their final mLE values increases with both W and κ, indicating the appearance of a mixed phase space. As the localisation of the normal modes increases, both the coupling between them and the value of the overlap integral $I_{\alpha\beta\gamma\delta}$ decrease, leading to a less chaotic system whose regions of regular motion (usually called stability islands) grow in size[1]. Larger stability islands imply that a larger fraction of chaotic orbits will be influenced by their presence, spending more time close to them, experiencing epochs of less chaotic behaviour, and therefore have a low mLE. The orbits that are in the chaotic sea are not influenced by this effect and therefore are still highly chaotic, leading to a larger spread of mLEs obtained within the sample.

To see how little the mLE tells us about the ergodicity of a trajectory, we now take a closer look at the four (W, κ)-combinations that have been marked in fig. 1. In fig. 2, we plot, for each of these parameter sets, the mLE *vs.* the time-averaged PF $\bar{\phi}$ of every run. Three regimes appear in the mLE-PF plot: for $\bar{\phi} < 0.1$, a wide range of mLE values occur for very similar $\bar{\phi}$; for $0.1 < \bar{\phi} < 0.5$, a weakly positive correlation exists between mLE and PF; and for

[1]Note that in the extreme case where nonlinearity vanishes the system becomes integrable, chaos is not present and the whole phase space is covered by stability islands (see, *e.g.*, sect. 1.3 of [42]).

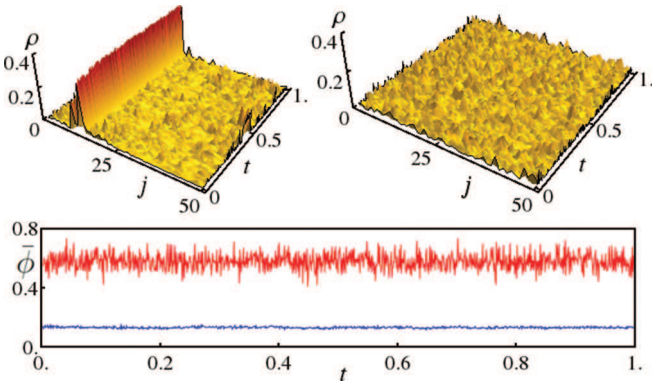

Fig. 3: (Colour on-line) The time evolution of the density and PF of two examples (marked in black boxes in fig. 2), with $W = 3$ and $\kappa = 1.4$. Time is plotted in units of $10^5\hbar/J$; j represents the site index, and ρ the unit-normalised density. The disorder and interaction strenghts are identical; the only difference is the disorder realisation, and hence the initial condition. The upper right panel shows the density evolution associated with the highest of the two PF values. The energies are $2.42J$ (upper right) and $0.36J$ (upper left). The initial condition is not shown, as it would obscure the view on the remainder of the evolution.

$\bar{\phi} > 0.5$, a higher $\bar{\phi}$ implies a lower mLE. The results for $\bar{\phi} < 0.1$ can be understood in terms of the above-mentioned stability islands. The high-$\bar{\phi}$ results present an intriguing topic for follow-up research. Finally, it is noteworthy that the positive correlation between mLE and PF that does exist for intermediate $\bar{\phi}$ is very weak.

The most important aspect of fig. 2 for the present discussion is that with the same W and κ, significantly different PFs occur for very similar mLEs, as exemplified by the two cases marked in black boxes (both have $W = 3$, $\kappa = 1.4$). The hypothesised connection between chaoticity and ergodicity would imply that chaotic systems should not be localised, so high mLEs should come with high participation numbers. While such behaviour is found in certain cases for intermediate PF values (between 0.1 and 0.5), fig. 2 shows that this is not the case at either low or high values of $\bar{\phi}$. We conclude that the mLE has very little predictive power when it comes to localisation.

Figure 3 shows the evolution of the density distribution and PF of the two trajectories marked with black boxes in fig. 2. The two trajectories have energies of $2.42J$ (upper left panel) and $0.36J$ (upper right panel). In one case, a large fraction of the density is stuck on a few sites, and the PF is correspondingly low. States with the same energy but very different density distributions are clearly possible —the peak could occur on different sites with similar potential energy, or be redistributed over sites with higher potential energy. The trajectory fails to reach such states, and is therefore clearly not ergodic, as also indicated by the absence of fluctuations in its PF evolution. This cannot be a classical (as opposed to Anderson) localisation effect, since the energy of the state is higher than the highest possible on-site potential. We conclude that the chaotic behaviour indicated by the mLE must be confined to a subvolume of the total allowed phase space. The other example does not have any preferred sites, and features much smaller peaks. The evolution of ϕ for this trajectory shows more fluctuations, indicating more variation in the states it visits, while remaining confined to a rather narrow band.

Discussion/conclusion. – The observed confinement of trajectories invites more discussion. In two degree-of-freedom Hamiltonian systems without escapes the stability islands separate the phase space in noncommunicating regions. Consequently isolated chaotic regions (often named chaotic seas) can occur. In higher-dimensional systems this separation is not possible, as the stability islands are tori whose dimensionality is not high enough to let them act as barriers between different regions ([42], sect. 1.4b). So, even in cases where the phase space of high-dimensional nonlinear systems is mostly occupied by stability islands, the remaining chaotic regions are interconnected. Consequently, each chaotic orbit can eventually visit every chaotic region in the phase space, although the time for this to happen might become extremely long. This phenomenon is called "Arnold diffusion" (see, for example, sect. 1.4 of [42] and sect. 2.11.14 of [43]), and allows for the theoretical possibility that the confined orbits we find will, at some point much later in time, escape from their region of confinement. However, such considerations are experimentally not relevant, due to the timescales involved. Effective ergodicity for physically relevant parameter values is then broken, as can be seen in, *e.g.*, the evolution shown in the upper left panel of fig. 3.

The results shown in fig. 2 provide a starting point for a more in-depth discussion of the various types of dynamics that can be expected in BECs in disordered potentials. The different regimes identified in the above discussion of fig. 2 are likely to have interesting physical explanations that shed more light on the behaviour of superfluids in the presence of disorder. We hope to inspire more research in this direction.

It would be interesting to compare our classical results to the predictions of an analogous quantum model. The closest quantum analogue of the DNLS is the Bose-Hubbard model, which yields the DNLS after a weakly interacting mean-field approximation. The most closely related quantum phenomenon would be many-body localisation; unfortunately, no consensus exists at present concerning its occurrence or nature, rendering such a comparison impossible at this stage.

In conclusion, we find that Anderson localisation-like effects break the connection between thermalisation and chaoticity in the disordered DNLS/mean-field Bose-Hubbard model. In particular, we have shown that the mLE fails to distinguish between trajectories which explore all energetically allowed areas of phase space and those confined to a subregion. In other words, the mLE *cannot* be used to determine the applicability of the

microcanonical ensemble to the disordered DNLS, unlike in the disorder-free case [10]. In order to predict thermalisation, the mLE has to be combined with some other suitably chosen quantity, such as the PF.

The reasoning that leads us to these conclusions is based on the strong connection between the themes of thermalisation and localisation: a trajectory that remains localised in general does not satisfy the ergodic hypothesis, and therefore cannot thermalise. The occurrence of localisation therefore allows us to come to very concrete conclusions about thermalisation. We find that some of these trajectories, in spite of their chaotic nature, do not uniformly explore all of the energetically available phase space. Since thermal predictions are based on the assumption of such exploration, *i.e.* ergodicity, we can safely say that those trajectories do not thermalise.

We conclude that although chaos is a necessary condition for ergodicity, it is not a sufficient one.

* * *

OT and AL thank Evangelos Siminos for inspiring discussions. ChS was supported by the Research Committees of the Aristotle University of Thessaloniki (Prog. No 89317) and the University of Cape Town (Start-Up Grant, Fund No. 459221).

REFERENCES

[1] Billy J., Josse V., Zuo Z., Bernard A., Hambrecht B., Lugan P., Clment D., Sanchez-Palencia L., Bouyer P. and Aspect A., *Nature*, **453** (2008) 891.
[2] Roati G., D'Errico C., Fallani L., Fattori M., Fort C., Zaccanti M., Modugno G., Modugno M. and Inguscio M., *Nature*, **453** (2008) 895.
[3] Damski B., Zakrzewski J., Santos L., Zoller P. and Lewenstein M., *Phys. Rev. Lett.*, **91** (2003) 080403.
[4] Anderson P., *Phys. Rev.*, **109** (1958) 1492.
[5] Schulte T., Drenkelforth S., Kruse J., Ertmer W., Arlt J., Sacha K., Zakrzewski J. and Lewenstein M., *Phys. Rev. Lett.*, **95** (2005) 170411.
[6] Lugan P., Clement D., Bouyer P., Aspect A., Lewenstein M. and Sanchez-Palencia L., *Phys. Rev. Lett.*, **98** (2007) 170403.
[7] Fisher M. P. A., Weichman P. B., Grinstein G. and Fisher D. S., *Phys. Rev. B*, **40** (1989) 546.
[8] Jaksch D., Bruder C., Cirac J. I., Gardiner C. W. and Zoller P., *Phys. Rev. Lett.*, **81** (1998) 3108.
[9] Kevrekidis P., Frantzeskakis D. and Carretero-González R., *Emergent Nonlinear Phenomena in Bose-Einstein Condensates* (Springer, Berlin) 2010.
[10] Cassidy A. C., Mason D., Dunjko V. and Olshanii M., *Phys. Rev. Lett.*, **102** (2009) 025302.
[11] Benettin G., Galgani G., Giorgilli A. and Strelcyn J.-M., *Meccanica*, **15** (1980) 9.
[12] Benettin G., Galgani G., Giorgilli A. and Strelcyn J.-M., *Meccanica*, **15** (1980) 21.
[13] Eckmann J.-P. and Ruelle D., *Rev. Mod. Phys.*, **57** (1985) 617.
[14] Skokos C., *Lect. Notes Phys.*, **790** (2010) 63.
[15] Molina M. I., *Phys. Rev. B*, **58** (1998) 12547.
[16] Pikovsky A. S. and Shepelyansky D. L., *Phys. Rev. Lett.*, **100** (2008) 094101.
[17] Kopidakis G., Komineas S., Flach S. and Aubry S., *Phys. Rev. Lett.*, **100** (2008) 084103.
[18] Flach S., Krimer D. O. and Skokos C., *Phys. Rev. Lett.*, **102** (2009) 024101.
[19] Skokos C., Krimer D. O., Komineas S. and Flach S., *Phys. Rev. E*, **79** (2009) 056211.
[20] Veksler H., Krivolapov Y. and Fishman S., *Phys. Rev. E*, **80** (2009) 037201.
[21] Mulansky M., Ahnert K., Pikovsky A. and Shepelyansky D. L., *Phys. Rev. E*, **80** (2009) 056212.
[22] Skokos C. and Flach S., *Phys. Rev. E*, **82** (2010) 016208.
[23] Flach S., *Chem. Phys.*, **375** (2010) 548.
[24] Laptyeva T. V., Bodyfelt J. D., Krimer D. O., Skokos C. and Flach S., *EPL*, **91** (2010) 30001.
[25] Bodyfelt J. D., Laptyeva T. V., Gligoric G., Krimer D. O., Skokos C. and Flach S., *Int. J. Bifurcat. Chaos*, **21** (2011) 2107.
[26] Bodyfelt J. D., Laptyeva T. V., Skokos C., Krimer D. O. and Flach S., *Phys. Rev. E*, **84** (2011) 016205.
[27] Basko D., *Ann. Phys. (N.Y.)*, **326** (2011) 1577.
[28] Vermersch B. and Garreau J. C., *Phys. Rev. E*, **85** (2012) 046213.
[29] Kottos T. and Shapiro B., *Phys. Rev. E*, **83** (2011) 062103.
[30] Bountis T. and Skokos H., *Complex Hamiltonian Dynamics*, *Springer Series in Synergetics* (Springer, Berlin) 2012.
[31] Kramer B. and MacKinnon A., *Rep. Prog. Phys.*, **56** (1993) 1469.
[32] Skokos C., Gerlach E., Bodyfelt J., Papamikos G. and Eggl S., arXiv:1302.1788 (2013).
[33] Gerlach E., Eggl S., Skokos C., Bodyfelt J. and Papamikos G., presented at the *10th HSTAM International Congress on Mechanics, 2013*, nlin.CD/1306.0627.
[34] Hairer E., Lubich C. and Wanner G., *Geometric Numerical Integration. Structure-Preserving Algorithms for Ordinary Differential Equations*, *Springer Series in Computational Mathematics*, Vol. **31** (Springer, New York) 2002.
[35] McLachan R. and Quispell G., *J. Phys. A*, **39** (2006) 5251.
[36] Forest E., *J. Phys. A*, **39** (2006) 5321.
[37] Contopoulos G., Galgani L. and Giorgilli A., *Phys. Rev. A*, **18** (1978) 1183.
[38] Skokos C. and Gerlach E., *Phys. Rev. E*, **82** (2010) 036704.
[39] Gerlach E., Eggl S. and Skokos C., *Int. J. Bifurcat. Chaos*, **22** (2012) 1250216.
[40] Greiner M., *Ultracold quantum gases in three-dimensional optical potentials*, PhD Thesis Ludwig-Maximilians-Universität München (2003).
[41] Chin C., Grimm R., Julienne P. and Tiesinga E., *Rev. Mod. Phys.*, **82** (2010) 12251286.
[42] Lichtenberg A. and Lieberman M., *Regular and Chaotic Dynamics*, second edition (Springer, New York) 1992.
[43] Contopoulos G., *Order and Chaos in Dynamical Astronomy*, *Astronomy and Astrophysics Library Series* (Springer, New York) 2002.